

Vortex liquid in single-crystal $\text{YBa}_2(\text{Cu}_{1-x}\text{Fe}_x)_3\text{O}_{7-\delta}$ of varying anisotropy

Yu. Eltsev and Ö. Rapp

Department of Solid State Physics, The Royal Institute of Technology, S-100 44 Stockholm, Sweden

(Received 1 December 1994; revised manuscript received 1 February 1995)

The vortex liquid has been studied in single-crystal $\text{YBa}_2(\text{Cu}_{1-x}\text{Fe}_x)_3\text{O}_{7-\delta}$ in magnetic fields up to 8 T parallel to the c axis both with a dc-flux transformer-contact configuration and by measuring the c -axis resistivity. With current along the ab planes, the c -axis resistance drops to zero and the voltages on different ab planes become equal at a temperature $T_{br}(B)$. With increasing anisotropy, $T_{br}(B)$ decreased in agreement with a recent theory by Daemen *et al.* for a Josephson-coupled layered superconductor. The results for current injection along the ab planes and along the c axis are consistent with anisotropic local conductors for all samples.

The vortex dynamics of high-temperature superconductors displays unusual features. One interesting question is the description of vortex motion and dimensionality in the liquid regime, above a vortex melting transition and below the thermodynamic critical field $B_{c2}(T)$. When a magnetic field [$>B_{c1}(T)$] is applied perpendicularly to the layers of a high- T_c superconductor, one can envisage flux lines as tubes moving under the Lorentz force with preserved shape. Alternatively vortices may decouple and move independently in different ab planes of the crystal in the form of a complicated entanglement and/or with the development of pancakelike two-dimensional vortices.

The use of multiterminal contacts on opposite ab planes is a powerful experimental technique to study these problems. In experiments with this configuration on $\text{Bi}_2\text{Sr}_2\text{CaCu}_2\text{O}_x$ (Bi-2212) single crystals,^{1,2} it was found that pancakelike vortices moving independently in different layers of the crystal were developed at all magnetic fields investigated, up to 5 T. Recently such experiments have been performed also in³⁻⁵ $\text{YBa}_2\text{Cu}_3\text{O}_{7-\delta}$ (Y-123). A magnetic-field-dependent temperature $T_{br}(B)$, was found, below which vortices preserve their integrity over the c -axis length of the sample. Above $T_{br}(B)$ vortices break up into thinner, quasi-two-dimensional objects with independent motion in different ab planes, similar to the observations in Bi-2212 crystals.

Alternatively the interlayer coupling can be probed by the c -axis resistivity. Daemen *et al.*⁶ considered a Josephson-coupled layered superconductor. They found that above a decoupling field, the critical current in the c direction is zero. This onset of c -axis resistivity was found by López *et al.*⁷ to roughly coincide with $T_{br}(B)$.

The possibility of nonlocal resistivity in the vortex liquid has also been pointed out.⁸ Recent experiments would seem to confirm this interpretation for Y-123 single crystals,³ in contrast to the results for Bi-2212 single crystals where all measured resistivities were well described by Montgomery-type analysis assuming local electrodynamics.^{1,2}

In the present paper we study the interlayer coupling in a series of Fe-doped Y-123 by current injections both in the ab plane and along the c axis. Fe doping allows for variation of anisotropy and makes it possible to compare the results in some detail with the theory of Daemen *et al.*⁶ The magnetic

field $B_{br}(T)$ where vortices lose their coherence over the c -axis length of the sample, was found to decrease with increasing anisotropy. The onset of c -axis resistivity was correlated with $B_{br}(T)$ for all samples.

Sample preparation was described previously.⁴ The Fe concentration was determined in an analytical scanning electron microscope, and the T_c was found to be in good agreement with results in the literature.⁹ The ab surface of the crystals was examined in an optical microscope under polarized light. The observations were consistent with those made by high-resolution electron microscopy.¹⁰ The usual twinned structure was observed for the undoped samples. At $x=0.065$ we could not observe any twins, and investigation with polarized light showed no in-plane anisotropy. This suggests the presence of a tweedlike microstructure on a scale below the resolution of an optical microscope. For the $x=0.035$ sample, we observed both twinned regions with reduced twin boundary separation and regions with apparent tweedlike microstructure. The contact configuration is shown in Fig. 1, and is the same as used by Safar *et al.*³

For anisotropic samples the resistivities must in general be calculated from a Laplace equation. We used the series expansion obtained by Busch *et al.*² for the solution of

$$\frac{d^2V}{\rho_{ab}dx^2} + \frac{d^2V}{\rho_c dz^2} = 0. \quad (1)$$

ρ_{ab} and ρ_c are the resistivities in the basal plane and along the c axis (z), respectively. However, the accuracy is limited by the small size of the crystals. Each contact strip was 0.1–0.15 mm wide leaving only about 0.2 mm between contacts 2 and 3 (6 and 7) for measuring voltages V_{23} (V_{67}). Therefore three independent methods were used to estimate resistivities from measured voltages and currents: (i) A solution to Eq. (1) was obtained for current through 1 and 4 (I_{1-4}). (ii) A corresponding solution was obtained from current

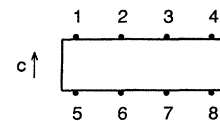


FIG. 1. Definition of contact arrangement.

TABLE I. Properties of $\text{YBa}_2(\text{Cu}_{1-x}\text{Fe}_x)_3\text{O}_{7-\delta}$ single crystals. ΔT_c is defined from 10–90 % of the resistance drop. The resistivities and resistivity ratios were evaluated at $1.1T_c$. γ was estimated from Eq. (2) as described in text.

Iron content	$x=0$	$x=0$	$x=0.035$	$x=0.065$
Thickness (μm)	160	63	13	6
$T_c(R=0)$ (K)	91	91	70	51
ΔT_c (K)	0.5	0.5	2.0	2.0
ρ_{ab} ($\mu\Omega\text{ cm}$)	67	69	56	79
ρ_c ($\text{m}\Omega\text{ cm}$)	2.0	2.7	42	235
ρ_c/ρ_{ab}	30	40	740	3000
$\gamma = \sqrt{m_c/m_{ab}}$		8	22	45

through 1 and 5 (I_{1-5}). (iii) Equation (1) was not applied. Nonuniform current distribution was minimized by estimating ρ_{ab} from V_{23} with currents I_{1-4} and I_{5-8} , and ρ_c from V_{26} with currents I_{1-5} , I_{3-7} , and I_{4-8} . The current was 1 mA in all measurements, well within the linear current-voltage region.

Sample properties are summarized in Table I. The results for the resistivities were obtained by method (i). The narrow transition widths in zero field indicate homogeneous samples. For both undoped samples we observed metalliclike temperature dependence of the normal-state in-plane resistivity ρ_{ab} as well as of the out-of-plane resistivity ρ_c , in agreement with recent results for Y-123 single crystals with optimal oxygen concentration.¹¹

The temperature dependence of ρ_{ab} and ρ_c in zero magnetic field for the Fe-doped samples is shown in the inset of the upper panel of Fig. 2. ρ_{ab} increases somewhat with Fe concentration and, for $x=0.065$, shows pronounced deviations from linearity above T_c . $\rho_c(T)$ is much more sensitive to the Fe content. The maximum value of ρ_c for the $x=0.065$ sample exceeds ρ_c for the undoped samples by a factor of about 100, approaching $\rho_c=1.5\text{ }\Omega\text{ cm}$, observed for Bi-2212 single crystal.¹²

Qualitatively the resistive properties of Fe-doped samples in zero magnetic field are similar to those observed for oxygen-deficient Y-123 single crystals.¹¹ The origin of a semiconductinglike $\rho_c(T)$ is still open. For our samples we cannot rule out that some variation in oxygen content contributes to the observed anisotropy in addition to Fe doping. However, for the context of the present paper, we note that a variation of the anisotropy can be controlled by our method, and defer a discussion of its detailed origin.

Figure 2 illustrates data obtained by method (iii) for the $x=0.035$ sample. In this and some subsequent figures only one of four samples is shown, but the results for all samples are similar (except for the strongly varying ρ_c). In all cases the magnetic field was oriented with $\mathbf{B}\parallel\mathbf{c}$. With decreasing temperature close to T_c , R_c goes through a maximum and starts to decrease at a lower temperature than R_{ab} . In zero magnetic field R_{ab} and R_c approach zero simultaneously, while for $B>0$, R_c falls sharply below the resolution limit of our instrument when R_{ab} is still >0 . The inset of the lower panel in Fig. 2 shows R_{ab} and R_c at $B=0$ and $B=2\text{ T}$ on logarithmic scales.

This behavior is qualitatively similar to observations in artificially layered MoGe/Ge materials¹³ with resistance an-

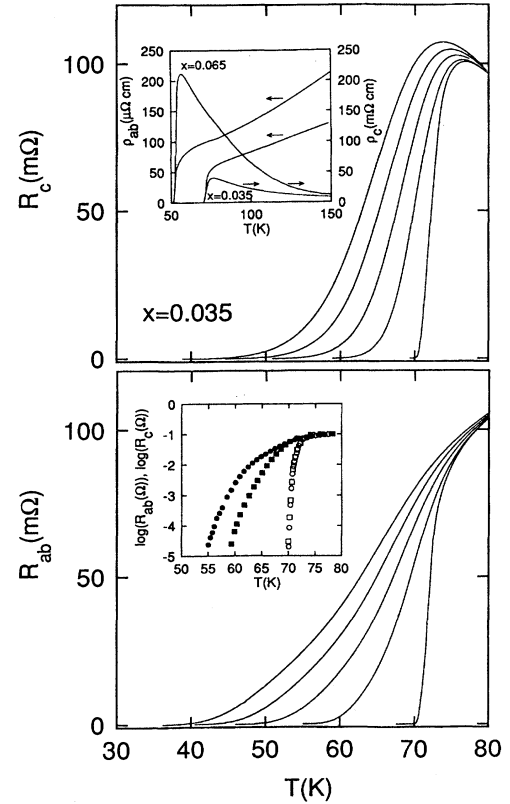


FIG. 2. Superconducting transition curves for $\text{YBa}_2(\text{Cu}_{0.965}\text{Fe}_{0.035})_3\text{O}_{7-\delta}$. Magnetic fields $\parallel\mathbf{c}$ are from right to left 0, 2, 4, 6, and 8 T in both panels. Inset top panel: Zero-field temperature dependence for the $x=0.035$ and 0.065 samples. Left-hand scale ab -plane resistivity, right-hand scale, c -axis resistivity. Method (iii) was used to estimate resistivities. Inset bottom panel: Basal plane and c -axis resistances for the $x=0.035$ sample at 0 and 2 T. Open symbols: $B=0$, closed symbols: $B=2\text{ T}$, squares: R_c , circles: R_{ab} . The logarithm in the inset is a base-10 logarithm.

isotropy of the order of 10^4 , where an abrupt drop of the out-of-plane resistivity at finite in-plane resistivity was linked with a buildup of interlayer phase coupling and the establishment of line vortices.

Another possibility to monitor the decoupling transition between layers is to measure the potential drops on different ab -plane surfaces of the crystal. Figure 3 illustrates the results at 2 T for the $x=0.035$ sample. With current I_{1-4} , voltages V_{23} , V_{67} , and V_{26} were measured. At low temperatures, the equal magnitude of V_{23} and V_{67} shows that vortices move with the same velocity in opposite ab planes of the crystal. Above T_{br} the stronger increase of V_{23} with increasing temperature indicates a larger velocity of the vortices on top of the crystal and a loss of vortex correlation along the c -axis direction due to thermal disorder.

In spite of the strongly inhomogeneous current distribution in the dc transformer-contact configuration, V_{26} roughly measures R_c . In fact, when V_{26} starts to increase from zero it is found to scale closely with the curve for R_c from Fig. 2. The results show that the smallest measurable R_c is found near $T_{br}(B)$, defined from $V_{23}>V_{67}$. In line with a recent theoretical prediction¹⁵ we thus find support for a region in

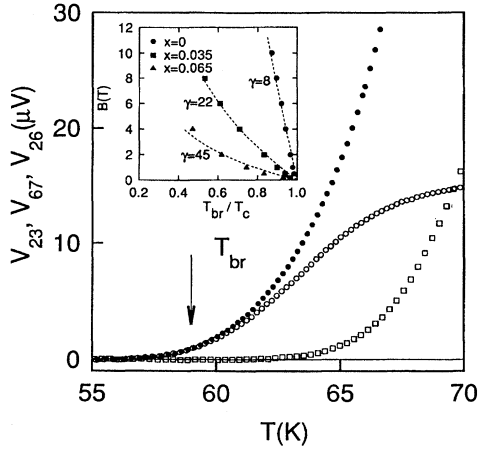


FIG. 3. Results for the $x=0.035$ sample at 2 T with $\mathbf{B}\parallel c$ and current through I_{1-4} . Full circles: V_{23} , open circles: V_{67} , open squares: V_{26} . The temperature T_{br} marks the onset of both c -axis resistance and the region where $V_{23} > V_{67}$. Inset: The magnetic-field dependence of T_{br} for three samples. The curves are calculations from Eq. (2) with γ as a free parameter.

the phase diagram above the irreversibility line $T_{irr}(B)$, where $\rho_c=0$ and $\rho_{ab}>0$. A similar temperature range $T_{irr}(B) < T < T_{br}(B)$ was found⁷ in pure Y-123 single crystals of varying thickness up to 60 μm .

With current in the ab planes, dissipation in the vortex liquid above the irreversibility line is due to motion of unpinned vortices under the Lorentz force. The absence of dissipation for current in the c -axis direction shows that the vortices remain relatively straight, preserving phase coherence between different layers. According to Daemen *et al.*⁶ the dissipation along the c axis is initiated with increasing temperature when the coherence is lost due to thermal disorder. In this picture we can thus associate the decoupling line of Ref. 6 with $B_{br}(T)$ observed in our experiment.

The inset in Fig. 3 shows the phase boundary $B=B(T_{br}/T_c)$ for samples of varying Fe concentration. The curves were calculated with the mass anisotropy ratio $\gamma = \sqrt{m_c/m_{ab}}$ as adjustable parameter from the expression for $B_{br}(T)$ for moderate anisotropy ($\gamma < \gamma_{cr} \approx 60$) given by Daemen *et al.*⁶

$$B_{br}(T) = \frac{\Phi_0^3}{4\pi^2 \mu_0 s e k_B T \lambda_{ab}^2(T) \gamma^2}. \quad (2)$$

Φ_0 is the flux quantum, s the interplanar distance, and $e=2.718\dots$. For λ_{ab} we take¹⁶ $\lambda(T) = \lambda_0 / \sqrt{1 - (T/T_c)^2}$ with $\lambda_0 = 1400$ \AA .

Our observations are well accounted for by this theory. Increasing anisotropy leads to a strong depression of $B_{br}(T)$ and some increase of the curvature in the accessible field range. The results for γ are in good agreement with other results. For Y-123 our value of $\gamma=8$ is in between previous results of¹⁷ 7.7 and¹⁸ 8.7. One can compare the present Fe-doped samples with magnetic measurements on crystals where anisotropy has been changed by varying oxygen concentration.¹⁸ From Fig. 5 of Ref. 18 one finds a γ slightly above 20 at $T_c=70$ K, and $\gamma \approx 55$ for $T_c=50$ K.

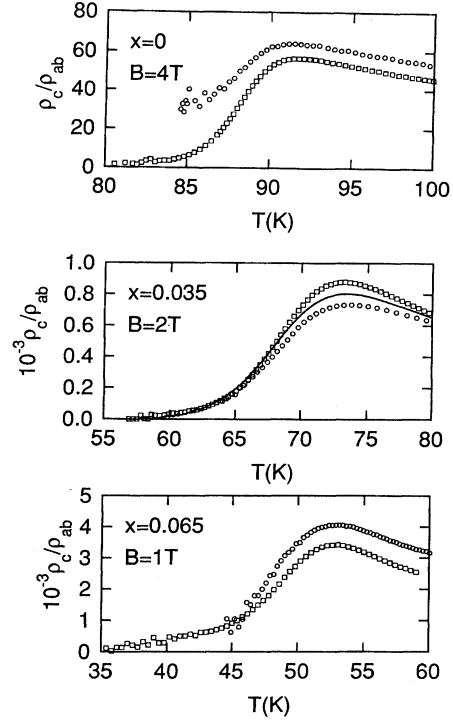


FIG. 4. ρ_c/ρ_{ab} for the $d=63$ μm undoped sample and two Fe-doped samples. Squares: data obtained by method (i), i.e., a solution to Eq. (1) with current through I_{1-4} . Circles: corresponding solution for current through I_{1-5} . The full line for the $x=0.035$ sample was obtained by method (iii). In all cases $\mathbf{B}\parallel c$, and of strengths given in the figure.

Both γ values are in fair agreement with our results for samples of corresponding T_c 's. It should be noted, however, that the model of Ref. 6 is based on c -axis conduction by Josephson tunneling between parallel planes, and it is not clear that this is the relevant mechanism for a relatively weakly anisotropic material such as the pure Y-123.

The results for the anisotropy can also be compared with the resistivity. Although ρ_c/ρ_{ab} is strongly temperature dependent in the region close to T_c , we can roughly assume that $\rho_c/\rho_{ab}(1.1T_c) \approx (m_c/m_{ab}) = \gamma^2$. From Table I it can be seen that this equality is obeyed to within 20% of the γ values obtained from Eq. (2), which is satisfactory considering this somewhat arbitrary choice of ρ_c/ρ_{ab} .

In the final part of the paper we shall show that measurements of ρ_c and ρ_{ab} in different contact configurations are consistent with a local anisotropic conductivity model. As described above, ρ_c drops faster to zero than ρ_{ab} , leading to $V_{67}/V_{23}=1$ below $T_{br}(B)$, when current is fed through I_{1-4} . By rotating the contact configuration one would then expect, in the local conductivity picture, that with current through I_{1-5} , measuring V_{26} and V_{37} , one would observe $V_{37}/V_{26} \rightarrow 0$ when $T \rightarrow T_{br}$ from above. However, in some recent experiments on Y-123 this was not the case. Instead $V_{37}/V_{26} \rightarrow 1$ when $T \rightarrow T_{br}$, as for the orthogonal configuration,³ implying that within local electrodynamics ρ_{ab} would go to zero faster than ρ_c . This contradiction therefore suggested nonlocal conductivity.

ρ_c/ρ_{ab} measured by different methods is shown in Fig. 4.

Methods (i) and (ii) give some different results, due to the uncertainty of geometrical factors. For the $x=0.035$ sample, method (iii) above was employed in addition. Values of ρ_c/ρ_{ab} in between those of the other methods were found, thus supporting the overall features of the results. Data for the undoped sample are more scattered than for the other samples since the resistivity is smaller, but suggest qualitatively the same conclusions. For all samples and all current injections ρ_c approaches zero faster than ρ_{ab} .

The gradual drop in the resistivity anisotropy near T_c leads to a significant difference between the original Giaever dc-flux transformer¹⁹ and its modification for high- T_c superconductors. In the former, current flows only through the primary film. Below T_c the voltage observed in the secondary film is due to motion of magnetically coupled vortices in both films under the Lorentz force acting only in the primary film. In the high- T_c pseudoflux transformer, the current injected from one ab plane of the crystal has a nonuniform distribution above T_{br} with a characteristic length² $z_{\text{eff}} \sim (\rho_{ab}/\rho_c)^{1/2}$. Near T_{br} , when ρ_c decreases faster than ρ_{ab} , z_{eff} diverges, current distribution becomes uniform, and voltages at top and bottom surfaces become equal. At $T < T_{br}$ the Lorentz force acting on the vortex line is the

same in different layers. Our results are qualitatively well described by this local picture.

The difference between our results and those of Ref. 3 are not understood. In our samples the twinning varies with Fe concentration. For $x=0.035$, the size of tweedlike and twinned regions was much smaller than the contact distances. Differences in twinning structure would therefore not seem to be the reason, but further investigations must be made for a more definite statement.

In summary we have varied anisotropy of Y-based 123 superconductors by doping with Fe. In all cases ρ_c drops faster towards zero than ρ_{ab} . The phase boundary for decoupled vortex motion in different ab layers of the crystals is found to be well described by Eq. (2). The resulting γ values were in agreement with results from oxygen-deficient 123 crystals of similar T_c values,¹⁸ suggesting a close relation between increasing anisotropy and T_c depression in Fe-doped and oxygen-deficient Y-123.

We are grateful to Z. Hegedüs for performing the elemental analysis of the Fe-doped samples. This work has been supported by the Swedish Superconductivity Consortium and by the Swedish Natural Science Research Council.

- ¹H. Safar, E. Rodriguez, F. de la Cruz, P. L. Gammel, L. F. Schneemeyer, and D. J. Bishop, Phys. Rev. B **46**, 14 328 (1992).
- ²R. Busch, G. Ries, H. Werther, G. Kreiselmeier, and G. Saeman-Ischenko, Phys. Rev. Lett. **69**, 522 (1992).
- ³H. Safar, P. L. Gammel, D. A. Huse, S. N. Majumdar, L. F. Schneemeyer, D. J. Bishop, D. López, G. Nieva, and F. de la Cruz, Phys. Rev. Lett. **72**, 1272 (1994).
- ⁴Yu. Eltsev, W. Holm, and Ö. Rapp, Phys. Rev. B **49**, 12 333 (1994).
- ⁵Yu. Eltsev, W. Holm, and Ö. Rapp, Physica C **235-240**, 2605 (1994).
- ⁶L. L. Daemen, L. N. Bulaevski, M. P. Maley, and Y. Coulter, Phys. Rev. Lett. **70**, 1167 (1993).
- ⁷D. López, G. Nieva, and F. de la Cruz, Phys. Rev. B **50**, 7219 (1994).
- ⁸D. A. Huse and S. N. Majumdar, Phys. Rev. Lett. **71**, 2473 (1993).
- ⁹E.g., J. M. Tarascon, D. Barboux, P. F. Miceli, L. H. Greene, and G. W. Hull, Phys. Rev. B **37**, 7458 (1988).
- ¹⁰Y.-W. Xu, M. Suenaga, J. Taftø, R. L. Sabatini, and A. R. Modenbaugh, Phys. Rev. B **39**, 6667 (1989).
- ¹¹K. Takenaka, K. Mizuhashi, H. Takagi, and S. Uchida, Phys. Rev. B **50**, 6534 (1994).
- ¹²C. Briceno, M. F. Crommie, and A. Zettl, Phys. Rev. Lett. **66**, 2164 (1991).
- ¹³D. G. Steel, W. R. White, and J. M. Graybeal, Phys. Rev. Lett. **71**, 161 (1993).
- ¹⁴Strictly a definition of T_{br} depends on a voltage sensitivity criterion (in our case 0.1 μV), above which differences in, e.g., V_{23} and V_{37} can be distinguished when current is fed through I_{1-4} . T_{br} thus increases somewhat with decreasing current. However, with the current at 1 mA, as used here, this effect is small. From comparison with F. de la Cruz, D. Lopez, and G. Nieva, Philos. Mag. B **70**, 773 (1994) we estimate 0.2–0.3 K.
- ¹⁵M. V. Feigelman, V. B. Geshenkbein, L. B. Joffe, and A. I. Larkin, Phys. Rev. B **48**, 16 641 (1993).
- ¹⁶W. N. Hardy, D. A. Bohn, D. C. Morgan, R.-X. Liang, and K. Zhang, Phys. Rev. Lett. **70**, 3999 (1993); J. Y. Lee, K. M. Paget, and T. R. Lemberger, Phys. Rev. B **50**, 3337 (1994).
- ¹⁷R. G. Beck, D. E. Farrell, J. P. Rice, D. M. Ginzberg, and V. G. Kogan, Phys. Rev. Lett. **68**, 1594 (1992).
- ¹⁸T. R. Chien, W. R. Datars, B. W. Veal, A. P. Paulikas, P. Kostic, Chun Gu, and J. Jiang, Physica C **229**, 273 (1994).
- ¹⁹I. Giaever, Phys. Rev. Lett. **15**, 825 (1965).